Recent Experimental Results on Orbital Electron Capture

BEROL L. ROBINSON,* *Department of Physics, Western Reserve University, Cleveland, Ohio*

AND

RICHARD W. FINK,† *Department of Chemistry, University of Arkansas, Fayetteville, Arkansas*

A summary is presented of experimental techniques and experimental results on electron-capture ratios, comparative half-lives, and transition energies. The effect of electron capture from the M shell and higher shells is taken into account. Transition energies are computed from the observed capture ratios for about twenty cases. A summary of mean L-fluorescence yields following nuclear excitation is brought up to date, and the origins of uncertainties in the interpretation of experimental results are discussed.

Six experiments are precise enough to be compared critically with the theory of Brysk and Rose, and the observed L/K capture ratios are found to be some ten percent greater than predicted. The discrepancies seem to be more or less independent of atomic number for $18 \leqslant Z \leqslant 53$; it is not at all clear that the effect of correlations between the coordinates of the K electrons, suggested by Odiot and Daudel, is sufficient to account for the discrepancy.

CONSIDERABLE experimental data have appeared since the publication in 1955 of a review[1] which compared experimental values of L/K capture ratios with the theoretical results of Brysk and Rose,[2] and which summarized our knowledge of transition energies involved in electron-capture decay and of mean L-fluorescence yields. The purpose of the present paper, therefore, is to present new data along the lines established previously.

I. EXPERIMENTAL TECHNIQUES

Essentially three fundamental techniques have been applied in the determination of x-ray intensity ratios and orbital electron-capture ratios.

A. External Source Spectrometry

The radioactivity is placed outside the sensitive volume, and the relative intensities of K and L x-rays are measured. Corrections must be applied for source self-absorption, self-scattering, and in some cases self-excitation of fluorescent x-rays (F5),‡ differential air and window absorption, and K- and L-fluorescence yields. One must also consider that a K-shell vacancy may be filled by an L electron either by radiative transition ($K_\alpha = K - L_{II}, L_{III}$) or by Auger transition ($K-LL$, or $K-LX$). The x-ray intensity ratio I_L/I_K is related to the capture ratio P_L/P_K by the expression

$$I_L/I_K = [(P_L/P_K) + n_{KL}]\bar{\omega}_L/\omega_K, \quad (1)$$

where $\omega_K = K$-fluorescence yield; $\bar{\omega}_L =$ mean L-fluorescence yield; and $n_{KL} =$ number of L-shell vacancies produced in the filling of a K-shell vacancy,

$$n_{KL} = k\omega_K + a_K\{[2(K-LL) + (K-LX)]/ [\Sigma \text{ Augers}]\}; \quad (2)$$

$k = I_{K\alpha}/I_K =$ intensity ratio of K_α x-rays to total K x-rays; $a_K = K$ Auger yield $= (1-\omega_K)$; and $(K-LX)$ = partial Auger yields; X denotes M-, N-, etc. shell electrons. $(K-LX)$ is the probability that a K-shell vacancy is filled by an L-shell electron with the excess energy carried off by an X-shell electron.

The value of n_{KL} was computed and displayed as a function of Z (Fig. 1, reference 1); the data available for this calculation have now been re-examined, and estimates have been made of the reliability of the results[3,4] (see Sec. IE and Fig. 1). The fraction of K x-rays in the K_α group, $(I_{K\alpha}/I_K)$, has been computed from the data in Compton and Allison[5] and other tabulations,[6,7] in the case of gallium a recent determination has been made by Drever and Moljk (D6), and Lazar (L15) has communicated recent measurements for some

* Supported in part by the National Science Foundation and the Department of Defense through the U. S. Air Force Office of Scientific Research.

† Supported in part by the National Science Foundation and the U. S. Atomic Energy Commission. Present address: The Gustaf Werner Institute for Nuclear Chemistry, University of Uppsala, Uppsala, Sweden.

[1] B. L. Robinson and R. W. Fink, Revs. Modern Phys. **27**, 424 (1955). Errata: Table I: E_{EC} of Mn^{54} should be 0.540 ± 0.010 Mev (p,n), *cc*. This makes no change in the capture ratios. Also a new measurement has been reported for Mn^{54}; $E_{EC} = 0.528 \pm 0.010$ *IB*(J4). Table II(b); K^{40} shoul dread (4− to 2+). Reference M4: change "1168" to "1186".

[2] H. Brysk and M. E. Rose, Oak Ridge National Laboratory Rept. ORNL-1830 (1955) (unpublished); Revs. Modern Phys. **30**, 1169 (1958).

‡ References in the text are in the form of numbered footnotes or initial-number combinations, e.g. (A2). The latter are also the references for the Tables and for Fig. 5, and are listed with the Tables.

[3] L. Slack and K. Way, *Radiations from Radioactive Atoms in Frequent Use* (U. S. Atomic Energy Commission, Washington, D. C., 1959), pp. 67–69.

[4] Wapstra, Nijgh, and van Lieshout, *Nuclear Spectroscopy Tables* (Interscience Publishers, Inc., New York, 1959), pp. 82–87. It may be noted that the f_{KL_i} estimated in these Tables, pp. 86–87, is connected with our n_{KL} by the relation $n_{KL} = \Sigma_i f_{KL_i}$.

[5] A. H. Compton and S. K. Allison, *X-Rays in Theory and Experiment* (D. Van Nostrand Company, Inc., Princeton, New Jersey, 1935), second edition, p. 637ff.

[6] Reference 4, pp. 80–81.

[7] A. E. Sandström, *Handbuch der Physik* (Springer-Verlag, Berlin-Göttingen-Heidelberg, 1957), Vol. XXX, p. 236.

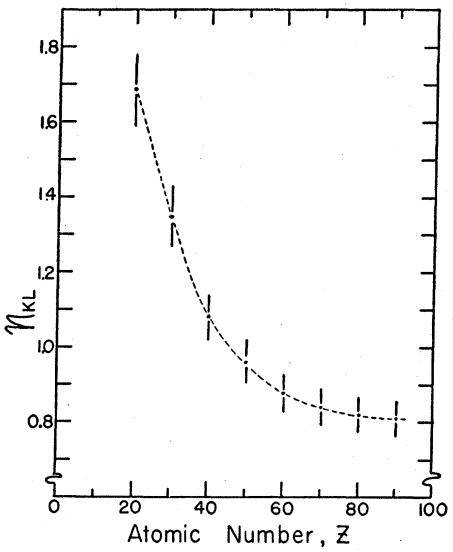

FIG. 1. n_{KL} is the number of L-shell vacancies produced in the filling of a K-shell vacancy.

elements between terbium and lead (see Sec. V). K-fluorescence yields are given by Broyles, Thomas, and Haynes,[8] Gray (G6), Laberrigue-Frolow and Radvanyi,[9] Roos,[10] and others. A recent summary of mean L-fluorescence yields has been given by Fink (F5) which is brought up to date in the present review. Trends in partial L-fluorescence yields and in Coster-Krönig yields are shown by Wapstra, Nijgh, and Van Lieshout.[4]

In some cases, all electron-capture transitions proceed via one excited state of the daughter. Then a measurement of the relative intensities or specific activities of the K x-ray and gamma ray will yield directly the fraction of captures from the K shell, P_K (H4, T3).

B. Internal Source Spectrometry

The radioactive material is dispersed throughout the sensitive volume of the detector. An advantage of this method is that a knowledge of the L-fluorescence yield is not required because the L radiations are (usually) totally absorbed in the counter.

The intensity ratio N_L/N_K of the L and K peaks may be measured directly in a gas proportional counter. The K peak arises from K Auger electrons and from K x-rays that are absorbed in the filling gas. The L peak comprises L Auger electrons and L x-rays following L capture as well as L radiation emitted after K capture, simultaneously with K_α x-rays that escape undetected from the counter. Neglecting L x-ray escape which is usually very small, the experimental capture ratio is given by (D6)

$$P_L/P_K=(N_L/N_K)(1-P\omega_K)-kP\omega_K, \qquad (3)$$

where P is the probability that a K x-ray can escape from the counter without being detected, and $k=I_{K\alpha}/I_K$ is the intensity ratio of K_α x-rays to total K x-rays, as in the foregoing.

In order to measure P_L/P_K experimentally, one chooses the dimensions of the counter and the type of filling gas so that the K x-ray escape probability P approaches either unity or zero, the former being experimentally simpler. However, if one chooses $P\rightarrow 1$, and uses a small low-pressure counter with a gas of low Z, such as methane or propane (L11, L12), the result depends critically upon ω_K. For example, for Ge^{71} Langevin[11] obtained $P_L/P_K=0.30$ using $\omega_K=0.45$; but if ω_K is taken to be about 0.50, this experiment gives $P_L/P_K=0.19$.

The alternative method, in which $P\rightarrow 0$, gives results independent of ω_K as shown by Eq. (3), and all radiations resulting from a K-capture or an L-capture event are integrated by the counter into the corresponding K or L peak, giving P_L/P_K directly, with an extremely small correction for K escape. The $P\rightarrow 0$ technique has been pioneered by Drever, Moljk, and Curran (D6, D7) who used an anticoincidence arrangement of two concentric proportional counters without an intervening wall ("wall-less" counter). An inner circle of wires acts as cathode for the central cylindrical proportional counter, while alternate anode and cathode wires in the outer annular region turn the surrounding layer of gas into a separate annular counter. With six atmospheres of argon-methane mixture containing radioactive $Ge^{71}H_4$ the probability that a 10.2-kev K x-ray escapes from the central counter and is not detected in the annular counter is less than 10^{-4}. The counting rate in the annular counter is some 15 times that in the central counter, which is 4.5 cm in diameter and has a sensitive length of 76 cm.

In another approach, scintillation crystals (M4) have been grown containing radioactive Cd^{109} and I^{125} (M5). The contribution of $L+M+\cdots$ capture was deduced from the difference between the number of K x-rays and the total number of gamma-ray transitions, under the assumption that one such transition, either photon or conversion electron, accompanies each decay. More recently, I^{126} has been produced by the reaction $I^{127}(\gamma,n)I^{126}$ in a crystal of NaI(Tl) introduced into the x-ray beam of a synchrotron (S12). In this case the K and L x-radiations were observed when the crystal was used as a scintillation spectrometer.

C. Coincidence Spectrometry

If electron-capture proceeds to an excited state of the daughter nucleus which in turn decays promptly by gamma-ray emission, then the branching probability for K capture P_K can be determined by a coincidence experiment. Let R_γ and $R_{K\gamma}$ be the counting rates for gamma rays and x-ray—gamma-ray coincidences, re-

[8] Broyles, Thomas, and Haynes, Phys. Rev. **89**, 715 (1953).
[9] J. Laberrigue-Frolow and P. Radvanyi, J. phys. et radium **17**, 944 (1956).
[10] C. E. Roos, Phys. Rev. **105**, 931 (1957).
[11] M. Langevin, Compt. rend. **239**, 1625 (1954).

spectively;

$$R_\gamma = D\epsilon_\gamma S_\gamma, \quad R_{K\gamma} = D\epsilon_\gamma S_\gamma P_K \omega_K \epsilon_K S_K,$$

and

$$R_{K\gamma}/R_\gamma = P_K \omega_K \epsilon_K S_K, \tag{4}$$

where D is the disintegration rate, S and ϵ are solid angles and intrinsic detection efficiencies of the counters, and ω_K is the K-fluorescence yield. The presence of internal conversion and other branches may complicate the analysis, but the result remains essentially unchanged (K4, B25). This technique is particularly useful for relatively complicated decay schemes, provided that there is a high-energy gamma-ray transition directly to the ground state or to a low-lying state. The most highly excited state will be populated by the electron-capture transition of the lowest energy, and this in turn is the most favorable circumstance for inferring the capture energy from the capture ratio. "Crystal summing" experiments as well as ordinary coincidence experiments can be analyzed in this way (G7, G9).

D. Capture from Higher Shells

One must distinguish between the experiments in which the L/K capture ratio is determined by observation of the L and K radiations, and those in which the ratio of K capture to total capture is measured, as in the coincidence experiments mentioned in (IC). In the latter cases one may readily deduce the ratio $(P_L+P_M+\cdots)/P_K \equiv P_{LM\ldots}/P_K$, and this value is frequently reported. Distinction will be made between these ratios in both the experimental and theoretical results reported in the following.

E. Uncertainties in the Interpretation of Experimental Results

The interpretation of the experiments on electron-capture requires knowledge of several auxiliary quantities from the domain of x-ray physics, and uncertainties in the latter are propagated into the results of the nuclear physics experiments.

In many experiments in which K x-rays are counted, a knowledge of the K-fluorescence yield is required. The best measurements to date are those of Roos,[10] which delineate the steeply rising portion of the ω_K *vs* Z curve for $26 \lesssim Z \lesssim 50$, and which are stated to some two or three percent. It would be of greatest value to know the K-fluorescence yields with a precision of one percent or better. Exact measurements and good agreement between the results of different experiments are especially lacking for $10 \lesssim Z \lesssim 25$, a region which contains some interesting cases, notably K^{40}.

In experiments in which both K and L x-rays are counted, one must take into account the L-shell vacancies produced in the filling of K-shell vacancies, a quantity called n_{KL} above. Re-examination of the data used in calculating n_{KL} leads to the assignment of uncertainties as shown in Fig. 1. For $Z \gtrsim 30$, the chief source of uncertainty lies in the K-fluorescence yield; if ω_K were known to one percent, then the uncertainty in n_{KL} would be halved. If in addition the ratio of the intensities of the K_α and K_β x-ray groups (which radiatively transfer the K-shell vacancies to the L shell and to higher shells, respectively) were known to one percent, then the uncertainty in n_{KL} would be halved again for $Z \gtrsim 50$; for $30 \lesssim Z \lesssim 50$, improved Auger yield measurements are also required. For $Z \gtrsim 30$, we need more precise knowledge of the total Auger yield (or, equivalently, the fluorescence yield, since $\omega_K + a_K \equiv 1$), and of the relative intensities of the $K-LL$, $K-LX$, and $K-XY$ groups of Auger electrons.

II. CALCULATED CAPTURE RATIOS

Table I is essentially a supplement to Table I of reference 1. It is slightly different in that (a) L_I and L_II capture are taken together, (b) capture from higher shells is computed, and (c) $\log f_n t$ is given for nth forbidden transitions with maximum spin change (the so-called unique transitions). The only nuclides repeated in Table I are Np^{235} and K^{40}, which are discussed in Sec. IV.

A. Capture from Higher Shells

The contribution of electron-capture from shells of principal quantum number greater than two is not negligible, and may be quite important in transitions of relatively low energy and in forbidden transitions.

As a zeroth approximation,[2] one might examine the nonrelativistic wave functions for a hydrogenlike atom.[12] The s-electron wave functions are proportional to $(Z/n)^{\frac{3}{2}}$, and thus the transition probabilities are proportional to n^{-3}. (This gives 0.125 for the $2s/1s$ ratio, a value which may be compared with the results of Brysk and Rose, which run from 0.08 for $Z=15$ to 0.16 for $Z=86$.) For p electrons the capture from shells with $n=2$, 3, 4, and 5 is found to be in the proportion 1:0.352:0.156:0.082.

As a somewhat refined approximation, Wapstra and Van der Eijk (W4) have used Slater screening constants in hydrogenlike wave functions. Alternatively, Ketelle, Thomas, and Brosi (K4) determined relative densities of M-, N-, etc., shell electrons from the results of the self-consistent field (SCF) calculations of Hartree and others.[13] Following the latter, we have calculated the total contribution to s-electron capture and p-electron

[12] See for instance L. Pauling and E. B. Wilson, Jr., *Introduction to Quantum Mechanics* (McGraw-Hill Book Company, Inc., New York, 1935), pp. 135–139.

[13] D. R. Hartree, Proc. Roy. Soc. (London) **A141**, 282 (1933), (Cl^-, Cu^+); D. R. Hartree, Phys. Rev. **46**, 737 (1934), (Hg^+); D. R. Hartree, Proc. Roy. Soc. (London) **A143**, 506 (1934), (Cs^+, K^+); D. R. Hartree and W. Hartree, Proc. Roy. Soc. (London) **A149**, 210 (1935), (Ca, Hg); Douglas, Hartree, and Runciman, Proc. Cambridge Phil. Soc. **51**, 486 (1955), (Au^+, Tl^+); W. G. Henry, Proc. Phys. Soc. (London) **A67**, 789 (1954), (Au^+); E. C. Ridley, Proc. Cambridge Phil. Soc. **51**, 702 (1955), (Mo^+).

TABLE I. New theoretical values of capture ratios calculated from known transition energies.

Z	A	Class	Half-life	E_{EC} (Mev) and method	References[a]	Initial state	Final state (Mev)	% EC	Log f_{0t}	Log f_{nt}	Theoretical capture ratios $(L_I+L_{II})/K$	L_{III}/K	L/K	$LM\cdots/K$	Remarks
19	K 40	B	1.3×10^9 y	0.043±0.008 *MS*, *cc* 0.060±0.008 (*p*,*n*)*cc*	G13 H15	4−	2+ 1.46	11%							See discussion of Sec. IV
27	Co 57	B	270 d	0.434±0.030 *IB* 0.755±0.030 (*p*,*n*)*cc*	J4 E2	7/2−	5/2− 0.136	∼100%	6.0 6.4		0.093			0.107	
33	As 74	A	18 d	2.55±0.02 β^+ 1.94±0.02 β^+	J6	2−	0+ ground 2+ 0.596	2% 38%	8.4 6.8	8.7	0.095 0.095	0.001	0.096	0.113 0.112	
37	Rb 84	A	33 d	2.65±0.01 β^+ 1.77±0.02 β^+, *cc* 0.75±0.02 *cc*	W6	2−	0+ ground 2+ 0.88 2+ 1.90	9% 66% 1.4%	8.1 7.0 7.9	8.6	0.101 0.102 0.103	0.001	0.102	0.111 0.121 0.122	
38	Sr 85	B	64 d	∼0.6 (est)	W7	9/2+	9/2+ 0.513	100%	6.2		0.108			0.130	
43	Tc 96	B	4.2 d	∼0.6 (est)	W8		2.42, 2.73		∼5.3		0.115			0.139	
51	Sb 119	A	38 hr	0.555±0.020 *IB*	O2	5/2+	3/2+ 0.024	∼100%	5.0		0.126			0.155	
53	I 126	A	13 d	2.13±0.02 β^+ 1.48±0.03 *cc* 0.73±0.04 *cc*	K9	2−	0+ ground 2+ 0.65 2+ 1.40	24% 27% 4%	7.8 7.5 7.7	8.0	0.125 0.123 0.128	0.004	0.129	0.158 0.151 0.157	
62	Sm 145	A	340 d	0.585±0.015 *IB* 0.160±0.015 *cc*	B25	7/2−	7/2+ 0.061 3/2+ 0.485	92% 0.0027%	7.8 11.3	8.8	0.151 0.41 0.23	0.34	0.75	0.189 0.99 0.29	 Forbidden Allowed
83	Bi 208g	C	3×10^4 y	0.31±0.08 (est)	F6, S14	4, 5+	3− 2.165	100%	12.4	(10.4)	0.545 0.302	0.163	0.71	0.92 0.39	Forbidden Allowed
84	Po 209	B	103 y	0.99±0.03 *cc*	F6, S14	1/2−	7/2− 0.91	∼5%	13.2	12.1	0.274 0.200	0.024	0.298	0.39 0.26	Forbidden Allowed
85	At 211	B	7.2 hr	$0.75<E_{EC}<0.82$ *cc*	F6, S14	9/2	ground	59%	6.0		0.215±0.002			0.31	
93	Np 235	A	410 d	0.13±0.02 *cc*	F6, S14	1/2+	1/2+ ground	∼100%	∼7		$11.3^{+\text{no limit}}_{-8.5}$			$16.3^{+\text{no limit}}_{-12.5}$	
94	Pu 237	A	46 d	0.21±0.02 *cc*	F6, S14	7/2−	5/2+ ground	60%	6.3		$0.86^{+0.30}_{-0.15}$			$1.19^{+0.38}_{-0.21}$	
				0.18±0.02 cc			7/2+ 0.033	22%	6.6		$1.4^{+1.0}_{-0.4}$			$1.90^{+1.4}_{-0.6}$	
				0.15±0.02 *cc*			5/2 0.060	15%	6.4		$3.0^{+20}_{-1.2}$			$4.2^{+23}_{-1.8}$	
97	Bk 245	A	4.98 d	0.59±0.02 *cc* 0.21±0.02 *cc*	F6, S14		0.25 0.63	4% 6%	7.0 7.0		0.32±0.01 $1.15^{+0.35}_{-0.26}$			0.42±0.01 $1.52^{+0.46}_{-0.35}$	

[a] See list at end of article.

capture from shells of $n \geqslant 2$. In Fig. 2 the results are given as the ratio of $(M+N+\cdots)/L$, neglecting the dependence on neutrino energy.

In the process of obtaining these results we had the opportunity to compare the density ratios of $2s$ and $1s$ electrons calculated by Brysk and Rose[2] with those obtained from the work of Hartree and his collaborators, whose nonrelativistic SCF results do not even approach the hydrogenlike value of 0.125, but range from 0.08 for $Z=20$ to 0.11 for $Z=80$. However, the value obtained from Mayers' relativistic SCF calculations for mercury[14] is 0.1485, in good agreement with the value of 0.150 which one reads from the graphical presentation of Brysk and Rose. On the other hand, there is good agreement between the relativistic and nonrelativistic SCF results for mercury for the ratios $3s/2s$, $4s/2s$, $3p/2p$, and $4p/2p$; and one is therefore led to have reasonable confidence in the validity of the results given in Fig. 2.

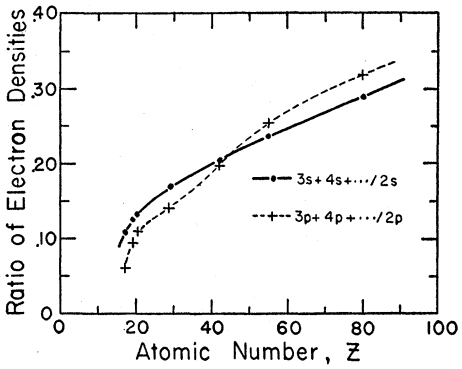

FIG. 2. Ratio of electron densities for $M+N+\cdots$ shells and L shell at the nuclear radius. Self-consistent field results for s electrons and p electrons.

B. Comparative Half-Life

As before, the logarithms of the comparative half-lives ($\log ft$) have been obtained from the nomograms of Moszkowski[15] or by the method given by Major and Biedenharn[16] in the case of low-energy transitions.

Davidson[17] has calculated and correlated $\log f_n t$ values for the nth forbidden unique beta decays. By analogy we have calculated $\log f_n t$ values for electron-capture transitions from the relations given by Major and Biedenharn[16] and by Brysk and Rose[2]:

$$ft=f_0 t=(\pi/2)g_K^2 q_K^2[1+(P_{LM}.../P_K)]t,$$
$$f_1 t=(\pi/24)g_K^2 q_K^4[1+(P_{LM}.../P_K)]t,$$

and

$$f_2 t=(\pi/2160)g_K^2 q_K^6[1+(P_{LM}.../P_K)]t. \quad (5)$$

For completeness we give here the $\log f_1 t$ values for the first forbidden unique transitions listed in reference 1: Ca^{41}, $\log f_1 t=9.4$; Tl^{204}, $\log f_1 t=8.4$. These two transitions, the ground state transitions of As^{74}, Rb^{84}, and I^{126}, and the weak inner transition in Sm^{145} all have $\log f_1 t$ values that are within the range of the $\log f_1 t$ values for this class of beta emitters tabulated by Feenberg,[18] although Ca^{41} is at the upper limit.

The $\log f_2 t$ value for the second forbidden unique transition of Po^{209} is also near the values calculated by Davidson[17] for Be^{10} and Na^{22}. On the basis of comparative half-life, one is tempted to classify the electron-capture of Bi^{208g} as second forbidden ($\Delta I=2$, no), but neither the half-life nor the transition energy is well enough known to permit any degree of assurance in this assignment.

C. Forbidden Transitions

Previously we discussed briefly the forbidden electron-capture transition of Ni^{59} ($\Delta I=2$, no; $\log ft=11.9$). For forbidden transitions with $\Delta I \geqslant 2$, the multiplicity of matrix elements precludes making precise connection between the energy of the transition and the capture ratios. Nevertheless some conclusions can be drawn from an examination of the expressions given by Brysk and Rose[2] in which g and f, the large and small parts of the Dirac wave function, are mixed.

(i) There is no effect on the L_I/K ratio for two reasons. In the first place, $(f_{LI}/f_K)^2=(g_{LI}/g_K)^2$. Secondly, the interference terms, which may be negative, are proportional to the neutrino energy q; but when q becomes large the energy dependence of the capture ratio virtually vanishes for all transitions.

(ii) The L_{III}/L_I ratio also depends on the matrix elements, and precise determinations of both the capture energy and the L_{III}/L_I ratio might serve to identify the matrix elements (or their ratio) in these transitions. This is equivalent to the shape fitting of beta-ray spectra of these classes of forbidden transitions. The cases in point are Ni^{59}, Tc^{97g}, and perhaps Bi^{208g}.

III. COMPARISON OF THEORY AND EXPERIMENT

In Table II we have compared experimentally determined capture ratios with those calculated from known transition energies (transcribed from Table I or from Table I of reference 1) for 15 cases. Table II corresponds to Table II(a) of reference 1 and includes the cases mentioned therein with the exception of Pd^{103}; the latest experimental results on Pd^{103} make the situation appear inconclusive at this time.[19]

It may be said that there appears to be gross agree-

[14] D. F. Mayers, Proc. Roy. Soc. (London) **A241**, 93 (1957), (Hg^+, relativistic).
[15] S. A. Moszkowski, Phys. Rev. **82**, 35 (1951); reproduced in part in reference (S14), pp. 597–600.
[16] J. K. Major and L. C. Biedenharn, Revs. Modern Phys. **26**, 321 (1954).
[17] Jack P. Davidson, Jr., Phys. Rev. **82**, 48 (1951).
[18] Eugene Feenberg, *Shell Theory of the Nucleus* (Princeton University Press, Princeton, 1955), Chap. V.
[19] Avignon, Michalowicz, and Bouchez, J. phys. et radium **16**, 404 (1955).

TABLE II. Comparison of theory and experiment.

Z	A	Experimental method and results: Method[a]	References[g]	P_L/P_K	$P_{LM}.../P_K$	Theoretical predictions: P_L/P_K	$P_{LM}.../P_K$	Remarks
18	A 37	$B(P$ small)	L11, K10	$0.092^{+0.010}_{-0.005}$, 0.102 ± 0.008		0.082		[h]
19	K 40	A[b]	H4					See Sec. IV for discussion
26	Fe 55	$B(P\to 0)$	S13	0.108 ± 0.006		0.097		[h]
27	Co 57	[c]	M12		0.20 ± 0.13		0.107	
32	Ge 71	$B(P\to 0)$	D6, D7	$0.128^{+0.005}_{-0.003}$		0.106		[h] This result is considered to supercede that given in reference D6
			D9	0.116 ± 0.005				
33	As 74	$B(P\to 0)$	S9	$0.085+0.020$		0.095		
36	Kr 79	$B(P$ not small)	L12	0.16 ± 0.03		0.101		[i]
		$B(P\to 0)$	D9	0.108 ± 0.005				[h]
37	Rb 84	C[d]	W6		0.12 ± 0.05		0.121	Capture to 0.89-Mev level
38	Sr 85	C[d]	B26		0.14 ± 0.05		0.130	Capture to 513-kev level; reported as $P_K=(88\pm4)\%$; theoretical value is 89%
53	I 126	$B(P\to 0)$[e]	S12	$0.142^{+0.005}_{-0.018}$		0.123		[h]
62	Sm 145	C[f]	B25		0.20 ± 0.02		0.189	Capture to 61-kev level
		C[d]			$0.6\ \pm0.1$		0.99	Forbidden transition to 485-kev level
							0.29	Allowed transition to 485-kev level
85	At 211	A	H8	0.143		0.215 ± 0.002		See also (G6)
93	Np 235	A	H10, G8	30 ± 2, 36.7 ± 4		$11.3^{+\text{no limit}}_{-8.5}$		[j]
94	Pu 237	A[e]	H14	2.8 ± 0.8		$+20$ $3.0-1.2$		Capture to 59.6-kev level; see Table III
97	Bk 245	C[d]	M13	~ 0.33		0.32 ± 0.01		Capture to 0.25-Mev level; see Table IV for L capture to 0.63-Mev level

[a] A, B, and C refer to external source, internal source, and coincidence spectrometry, respectively; P is the probability that a K x-ray escapes from the counter in internal source spectrometry.
[b] Specific activity for K x-rays and gamma rays.
[c] Beta-ray spectrometry of Auger and internal conversion electrons.
[d] K x-ray—gamma-ray coincidences.
[e] K and L radiation coincident with gamma-ray.
[f] K x-ray—L conversion electron coincidences.
[g] See list at end of article.
[h] These precision experiments are discussed in Sec. III and summarized in Fig. 3.
[i] This experimental result is critically dependent on the value chosen for K-fluorescence yield, as shown in the following table.

ω_K	0.57	0.60	0.63
P_L/P_K	0.26	0.16	0.10

[j] See Table III; see Table IV for M capture.

ment between theory and experiment. The apparent discrepancies in the cases of K^{40}, At^{211}, and the inner branch of Sm^{145} can in all likelihood be attributed to insufficiently precise data; and the result of Langevin for Kr^{79} (L12) depends critically upon the K-fluorescence yield. However, the precision measurements for A^{37}, Fe^{55}, Ge^{71}, Kr^{79}, and I^{126} are not in accord with the predictions of the theory of Brysk and Rose.[2] The six experimental results which are precise enough for critical comparison with the predictions of Brysk and Rose[2] are summarized in Fig. 3. The correction proposed by Odiot and Daudel[20] for A^{37} is also indicated in Fig. 3.

There appears to be a small but consistent discrepancy of some ten percent between these precision experimental measurements and the theoretical results of Brysk and Rose. Brysk has informed us that the latter were not intended to be more precise than a few percent.[21]

A. Correlations

Odiot and Daudel[20] have treated the problem of electron capture for small Z, taking into account the correlations that exist between the positions of the electrons. These arise from the facts that (i) the wave functions are not the same before and after capture, since the nuclear charge has changed by one unit, (ii) the wave functions must be antisymmetric in the coordinates of the electrons (Pauli exclusion principle), and (iii) the mutual repulsion of the K electrons may not be completely negligible compared to the attraction of

[20] S. Odiot and R. Daudel, J. phys. et radium **17**, 60 (1956).

[21] H. Brysk (private communication 1959).

the nucleus. (The latter is in a fashion taken into account by Brysk and Rose[2] in their use of screened wave functions.) Using nonrelativistic wave functions, Odiot and Daudel found that these considerations operate to suppress the capture of K electrons relative to L electrons by some 25% for $Z=18$.

The effect increases rapidly as Z decreases. Because reasonably exact wave functions are available, Odiot and Daudel made complete calculations for $Z=2$, although they are only of theoretical and academic interest since there are no L electrons in the ground state of helium, to say nothing of the fact that helium has no electron-capturing isotopes. At any rate, the capture ratio, P_L/P_K, is found to be increased tenfold for helium, while less exact calculations indicate that the increase is about threefold for $Z=4$. Unfortunately $_4Be^7$ seems to be quite inaccessible to experimental verification; however, some of the other low-Z electron-capturers ($_9F^{18}$, $_{11}Na^{22}$, $_{13}Al^{26}$, and $_{17}Cl^{36}$) would be worth study, although the experiments would be exceedingly difficult.

On the other hand, the effect falls off rapidly as Z increases, and although it was plainly insufficient to account for the large discrepancy previously ascribed[11] to $_{32}Ge^{71}$, it may perhaps account for the small discrepancies found in the recent precision experiments.

B. Discussion of Cases in Table II

Argon-37.—The effect of correlations has been calculated only for this case,[20] and it appears to increase the theoretical value of P_L/P_K from 0.080 to 0.100. The experimental values lie between these two numbers, but might be said to be in slightly better agreement with the latter than with the former.

Krypton-79.—The experiments of Langevin (L12) were performed under circumstances which make the results strongly dependent on the correction for the escape of K x-rays from the sensitive volume of the counter, and upon the value chosen for the K-fluorescence yield of bromine, as indicated in footnote (e) of Table II. Using the "wall-less" counter, Drever (D7, D9) has found a capture ratio for Kr^{79} which is in gross agreement with the theory of Brysk and Rose.

Astatine-211.—The experimental results on At^{211} are reported only as the ratio of the K and L x-ray intensities: $I_K/I_L=3.1$. This appears to be the result of absolute measurements of the K and L x-ray intensities in scintillation and proportional counter spectrometers, respectively; but there is little description of the experimental work which one might base an estimate of the precision of the intensity ratio quoted.

IV. TRANSITION ENERGIES DEDUCED FROM EXPERIMENTALLY DETERMINED CAPTURE RATIOS

Despite this rather uncertain situation as regards the detailed reliability and validity of the theory of electron capture, we proceed to Table III, in which are listed some capture energies which were calculated from experimentally determined capture ratios. We feel some confidence in these calculations because they lie in the relatively high-Z region for which we might expect any discrepancy to be small, and because most of the transition energies are found to be quite small and therefore are not very sensitive to small changes which may have to be made in the theory of electron capture. The case of K^{40} discussed in the following is a somewhat extreme example.

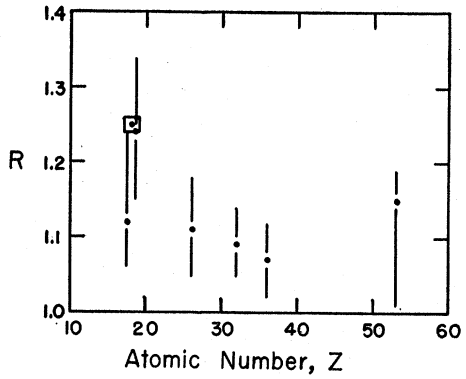

FIG. 3. $R=\dfrac{\text{experimentally observed } L/K \text{ capture ratio}}{\text{theoretical } L/K \text{ capture ratio of Brysk and Rose}}$.

The open square at $Z=18$ represents the correlation effect computed by Odiot and Daudel (reference 20). The uncertainty in R indicated by the length of the vertical bars does not include about 4% uncertainty in the theoretical results of Brysk and Rose.

Table III supercedes Table II(b) and Table IV of reference 1. The results for Cd^{109}, I^{125}, and W^{181} are merely repeated; there are new experimental results for Ba^{133}, Os^{185}, Au^{195}, and Tl^{202}, and twelve other radioactivities; K^{40} is also included, although the experimental results for this case are somewhat contradictory as will be discussed in the following in detail.

We have also calculated logft values for the transitions in Table III. With the exception of K^{40}, Tc^{97g}, La^{138}, and Er^{165}, the comparative half-lives seems to correspond to allowed or first forbidden transitions, that is, $|\Delta I|=0$ or 1. The low value obtained for Er^{165} is not understood; Tc^{97g} is a second forbidden transition ($\Delta I=2$, no) and its comparative half-life is in the range of the beta decays listed by Feenberg[18]; the other two exceptions are discussed below.

Table IV lists six pure or predominantly L-capture transitions. Some of the transition energies are established only between K- and L-ionization energies as limits. We have calculated logft values for the two cases in which the energy is rather well known, and estimated logf_1t for Pb^{202}; the latter value falls within the range of logf_1t values for other first forbidden unique transitions.

Several cases occur in both Table I and Tables III or IV. In Table I auxiliary information is used to determine or to estimate the transition energies, and capture ratios are computed. In Tables III and IV the argument

TABLE III. New decay energies from capture ratios.

Z A	Experimental method[a]	Initial state	Final state (Mev)		Experimental results: % EC	L/K	LM···/K	References[h]	Calculated E_{EC} (Mev)	Half-life	Log f_{0t}	Remarks
19 K 40	A[b]	4−	2+	1.46	11%					1.3×10⁹ y		i
43 Tc 97g	A[c]	9/2+	5/2+	Ground	100%	$0.21^{+0.14}_{-0.10}$		K8	$0.185^{+\text{no limit}}_{-0.065}$	2.6×10⁶ y	12.5	j
48 Cd 109	A[b]	5/2+	7/2+	0.088	100%	0.124±0.04	0.24±0.04	W4	0.078±0.010	470 d	5.1	
50 Sn 113	C[d]	1/2 or 3/2+	1/2 or 3/2+	0.650	3.5%		$2.23^{+1.12}_{-0.88}$	B24	$0.036^{+0.004}_{-0.001}$	119 d	5.0	
53 I 125	B[e]	5/2+	3/2+	0.0353	100%	0.23±0.03		M5	$0.108^{+0.020}_{-0.010}$	60 d	4.7	
56 Ba 133g	C[d]	1/2+	1/2+	0.437	~95%		$1.17^{+0.26}_{-0.20}$	G10	0.054±0.003	7.5 y	5.8	
57 La 138	A[b]	5+	2+	1.43	60%		1.4±0.25	T3	0.185±0.015	1.1×10¹¹ y	18.1	i, i $\log f_{2t}=12.9$
58 Ce 139g	B[e]	3/2+	5/2+	0.166	100%		0.37±0.02	K4	0.104±0.006	140 d	5.3	
61 Pm 145	C[f]	5/2+	3/2−	0.067	9%		0.85±0.03	B25	0.073±0.010	18 y	7.7	
64 Gd 153	C[d]	7/2−	7/2+	0.104	~100% ~75%		0.68±0.02 0.34±0.03	B13 G12	0.092±0.002 0.149±0.010	236 d	5.6 6.0	k
66 Dy 159	A[g]			Excited		1.0±0.3		G11	$0.079^{+0.010}_{-0.005}$	134 d	5.1	l
68 Er 165	A[g]	7/2−		Excited		1.2±0.4		G11	$0.082^{+0.010}_{-0.005}$	10 h	3.7	
73 Ta 179	A[g]	7/2+	9/2+	Ground	100%	1.4±0.4		B15	$0.094^{+0.009}_{-0.004}$	600 d	6.2	
74 W 181	A[g]		7/2+	Ground	100%	1.54±0.10		B5	0.092±0.009	140 d	5.5	m
76 Os 185	C[d]	1/2−	3/2+	0.87	17%		1.08±0.04 1.04±0.04	B17 J5	0.110+0.005	93 d	6.7	
79 Au 195	C[d]	3/2+	5/2−	0.128	~50%		5.5±0.9	B27	0.094±0.002	192 d	7.2	j
79 Au 196	C[d]	2−	2+	0.69	25%		0.41±0.12	G9	$0.234^{+0.180}_{-0.050}$	5.6 d	6.1	j
81 Tl 202	C[d]	2−	2+	0.44	61%		0.56±0.04	H13, G7	0.197±0.007	12 d	5.9	j
93 Np 235	A[g]	5/2+	7/2−	Ground	>98% ~100%	30±2 36.7±4		H10 G8	0.130 0.123±0.001	410 d	7.1	
94 Pu 237	A[g]	7/2−	5/2−	0.059	15%	2.8±0.8		H14	$0.153^{+0.010}_{-0.005}$	46 d	6.8	

[a] A, B, and C refer to external source, internal source, and coincidence spectrometry, respectively.
[b] Specific activity for K x-rays and gamma rays.
[c] K and L x-ray intensities from a solid source inside a proportional counter. This transition was compared to electron capture in Tc^{96}, but the results are quite insensitive to uncertainties in the decay scheme of the latter.
[d] K x-ray—gamma-ray coincidences.
[e] 4π scintillation counter ($P \to 0$).
[f] K x-ray—conversion electron coincidences.
[g] K and L x-ray intensities.
[h] See list at end of article.
[i] See detailed discussion in Sec. IV.
[j] E_{EC} (re)calculated by the authors of this paper.
[k] More complicated decay schemes are reported by M15 and M16; see also B18 for another report.
[l] See Table IV for L capture to an excited state. A detailed elucidation of this decay scheme is reported by K11.
[m] More complicated decay schemes are reported by D8 and C5.

is inverted, and observed capture ratios are used to determine transition energies. In the cases of Bk^{245}, Pu^{237}, and Np^{235}, the transition energies deduced from capture ratios are in agreement with the energies deduced from other data, within the limits of uncertainty assigned. Indeed, because of the steepness of the curve of capture ratio *vs* transition energy near the *K*-capture threshold, modestly well-determined capture ratios serve to define the transition energy with precision, e.g., Np^{235}.

Potassium-40.—The decay scheme and decay constants of naturally occurring K^{40} have been the subject of an unusual amount of interest primarily because of its geochronological importance. The decay scheme suggested by Morrison[22] has been confirmed and is generally accepted. The nuclear spin of K^{40} has been measured[23] and is found to be 4, and odd parity is assigned according to the shell model.[24] The ground states of Ca^{40} and A^{40} are of course 0+. The 1.328 ±0.010-Mev beta decay of K^{40} has a unique shape which is characteristic of a third forbidden transition ($\Delta I=4$, yes).[25] The electron capture of K^{40} proceeds (almost) entirely through the first excited state of A^{40} which is of course believed to be 2+. Helm[26] has questioned this assignment on the basis of experiments on the inelastic scattering of 187-Mev electrons from argon, but his alternative assignment of 0+ cannot apply to the state which undergoes a radiative transition to the 0+ ground state. It is generally concluded that the electron-capture is a first forbidden unique transition ($\Delta I=2$, yes).

Mass spectrometric and particle reaction results appear in Table I. Giese and Benson (G13) have compared the doublets $A^{40}-(C_3H_4)$ and $K^{40}-(C_3H_4)$ in a high-resolution mass spectrometer, and find that the mass difference corresponds to 1505±3 kev. It may be mentioned in passing that their result for the $K^{40}-Ca^{40}$ mass difference is 1320±3 kev, in good agreement with the beta-decay results. Holland and Lynch (H15) have observed neutron spectra of the reaction $A^{40}(p,n)K^{40}$, and obtain an energy difference of 1522±6 kev. The origin of this discrepancy is not known.

There are a number of reports of the energy of the K^{40} gamma ray, and an average value of 1462±5 kev has been adopted by Endt and Braams,[27] although it may be noted that they frequently refer to the "level at 1.48±0.02 Mev." If one combines the gamma-ray energy adopted by Endt and Braams with the mass spectrometric and particle reaction results, one obtains "closed cycle" values of 43±8 and 60±8 kev, respectively, for the capture energy of K^{40}.

[22] P. Morrison, Phys. Rev. **82**, 209 (1951).
[23] Davis, Nagle, and Zacharias, Phys. Rev. **76**, 1068 (1949); J. R. Zacharias, Phys. Rev. **61**, 270 (1942).
[24] Reference 18, p. 32, for instance.
[25] L. Feldman and C. S. Wu, Phys. Rev. **87**, 1091 (1952).
[26] R. H. Helm, Phys. Rev. **104**, 1466 (1956).
[27] P. M. Endt and C. M. Braams, Revs. Modern Phys. **29**, 683 (1957).

TABLE IV. *L*-capture transitions (pure or almost pure *L* capturers).

Z	A	Half-life	Initial state	Final state	Observed capture ratios L/K	Observed capture ratios M/L	References[a]	E_{EC}(kev)	Remarks
66 Dy	159	144 d	3/2 or 1/2−	5/2 or 3/2+	350 kev	$\lesssim 10$	K11	$9<E_{EC}<54$	350-kev gamma ray is not in coincidence with *K* x-rays
78 Pt	193g	~500 y	3/2 or 1/2−	3/2+	Ground	>1000	N1	$13<E_{EC}<77$	Only *L* x-rays were observed
82 Pb	202	3×10^5 y	0+	2−	Ground	>200	~0.40	H5	$15<E_{EC}<86$	Observed P_M/P_L implies that E_{EC} is well above lower limit; $\log ft\geqq 9.3$
82 Pb	205g	$\sim 2\times10^7$ y	5/2−	1/2+	Ground	>1600		W5	$15<E_{EC}<86$	Only *L* x-rays were observed; $E_{EC}\leqq 110$ kev (calculated with neutron binding energies, F6)
93 Np	235	410 d	1/2+	1/2+	Ground	36.7±4	0.46±0.05	G8, H10	123±1	Observed P_M/P_L gives $g_M^2/g_L^2=0.35\pm0.04$, which may be compared with 0.32 (Fig. 2); $\log ft=7.1$
97 Bk	245	4.98 d			630 kev			M13	185±15	$P_L=0.48$ (±~0.05); $P_K\geqq 0.1$; these observations are consistent with E_{EC} given here and $P_{MN\ldots}/P_L=0.4$; see Table I and Fig. 2; $\log ft=7.0$

[a] See list at end of article.

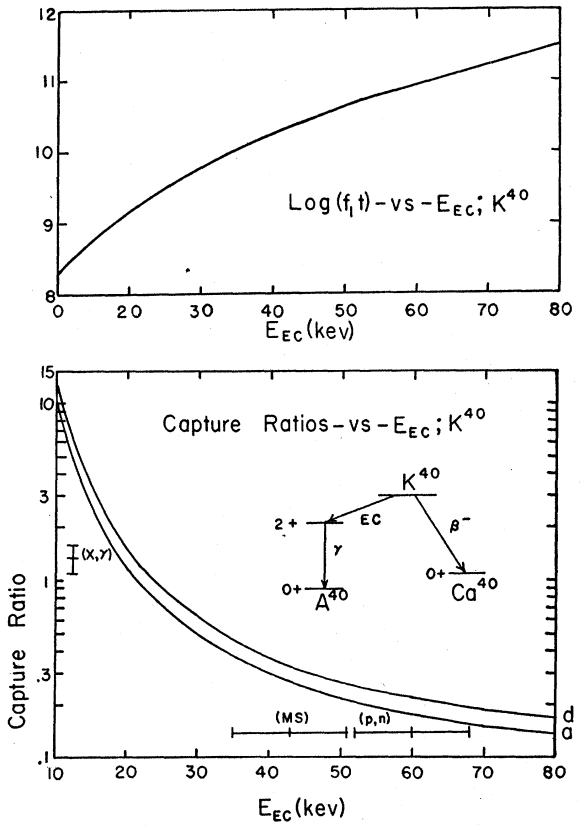

FIG. 4. (top) Comparative half-life of K^{40} *vs* capture energy for a second forbidden unique transition. (bottom) Electron capture ratio *vs* transition energy for K^{40}. (*a*) L/K ratio, Brysk and Rose (reference 2); (*b*) LM/K ratio (reference 2 and Sec. IIA); (*c*) L/K ratio including effects of correlations, Odiot and Daudel (reference 20); (*d*) LM/K ratio including correlations (reference 20 and Sec. IIA). (Curves *b* and *c* are omitted from the drawing but are approximately uniformly spaced between curves *a* and *d*.) [The spin of K^{40} is 4 and the parity is odd.]

The discussion can best be continued in terms of Fig. 4, in which we have plotted some curves of capture ratio *vs* transition energy for this first forbidden unique transition. The curves *a* to *d* are the following: (*a*) L/K capture ratio[2]; (*b*) LM/K capture ratio (reference 2 and Sec. IIA); (*c*) L/K capture ratio including the effects of correlations as calculated by Odiot and Daudel[20] for A^{37}; and (*d*) LM/K capture ratio including the effects of correlations (reference 20 and Sec. IIA). (Curves *b* and *c* have been omitted from the drawing in the interest of clarity, and lie approximately uniformly spaced between curves *a* and *d*.) The closed cycle values of the electron-capture energy are indicated by the bars along the energy axis.

Heintze (H4) determined the value of P_K from the specific activity of potassium for the emission of K x-rays and gamma rays. The capture ratio, $P_{LM}/P_K = 1.35 \pm 0.25$, is indicated by the bar along the capture ratio axis of Fig. 4. In obtaining this value Heintze measured the K-fluorescence yield of argon in an auxiliary experiment[28] and found $\omega_K = 0.13$. The transition energy inferred from Heintze's capture ratio is 20 ± 3 kev. Although the fluorescence yields obtained by Heintze[28] for higher-Z noble gases are a trifle larger than those reported by others[10] for neighboring elements, it would seem unlikely that the over-all error in P_K is large enough to lead to an appreciable change in the inferred capture energy, especially in view of the steepness of the curves of Fig. 4 in this region.

Figure 4 also contains a plot of $\log f_1 t$ *vs* transition energy for K^{40}. Feenberg[18] finds that first forbidden unique beta transitions have $7.5 \lesssim \log f_1 t \lesssim 9.5$, and we find a similar range for this class of electron-capture transitions (see Sec. IIB). The energy obtained from the capture ratio leads to a value of $\log f_1 t$ in this range; the other energies do not.

If the argument is now inverted so that one accepts 20 ± 3 kev as the electron-capture energy, and 1505 ± 3 kev (*MS*) or 1522 ± 6 kev (*p*,*n*) for the mass difference; then the separation between the ground state and the first excited state of A^{40} is 1485 ± 5 kev (*MS*) or 1502 ± 7 kev (*p*,*n*). The former value is not badly in disaccord with most of the measurements of the K^{40} gamma-ray energy.

Lanthanum-138.—The nuclear spin of La^{138} has been measured[29] to be 5, and even parity is assigned by the shell model. La^{138} undergoes a beta transition to the first excited state of Ce^{138} at 0.81 Mev, and an electron-capture transition to the first excited state of Ba^{138} at 1.43 Mev (T3). The gamma rays are assigned by their appearance in the spectra of Pr^{138} and Cs^{138}, respectively; furthermore, in the elucidation of the decay scheme of La^{138}, it was shown that the 1.43-Mev gamma ray is coincident with the barium K x-ray. Turchinetz and Pringle (T3) also determined the specific activity of La^{138} for barium K x-rays and for gamma rays, and found the capture ratio to be $P_{LM}.../P_K = 1.4 \pm 0.25$. We have recalculated the transition energy for a second forbidden unique transition ($\Delta I = 3$, no) including the effect of capture from higher shells, and find that the capture energy is 185 ± 15 kev. However we are unable to include the contribution of d electrons, and this transition energy may be too small. $\log f_2 t$ is 12.9, and it is comparable to other transitions of this class.[17]

Samarium-145.—As a final indication of the applicability of electron-capture theory, we turn to the experiments (B25) on the decay scheme of Sm^{145}. The electron capture proceeds predominantly through the 61-kev state of the daughter, and the energy of this transition has been measured by observing the inner bremsstrahlung of electron capture. There is a very weak branch to a highly excited state of the daughter, and the capture energy of this branch can be calculated from the decay scheme. By coincidence technique the capture ratio is measured for this weak low-energy transition. Comparing it with theoretical predictions for various

[28] J. Heintze, Z. Physik **143**, 153 (1955).
[29] P. B. Sogo and C. D. Jeffries, Phys. Rev. **99**, 613 (1955).

TABLE V. Recent measurements of L-fluorescent yields.

Z	$\omega_{L\text{III}}$	$\omega_{L\text{II}}$	$\omega_{L\text{I}}$	$\bar{\omega}_L$	K_β/K_α	References[a]	Method of excitation
65 Tb				0.19	0.22	L15	Electron capture
70 Yb				0.20	0.24		
72 Hf				0.24	0.25		
80 Hg				0.34	0.29		
81 Tl				0.37	0.29		
82 Pb				0.385	0.29		
73 Ta	0.23±0.02	0.23±0.04	0.28±0.07			R6	Monochromatic x-rays
78 Pt	0.275±0.03	0.31±0.04	0.35±0.08				
79 Au	0.32±0.03	0.27±0.04	0.36±0.09				
82 Pb	0.35±0.04	0.24±0.04	0.37±0.09				
80 Hg	0.34±0.01	0.42±0.09		0.371±0.035		H16	Internal conversion in Au^{199}
80 Hg				0.34±0.04		S10	Electron capture in Tl^{204}
81 Tl	0.33±0.02			0.32±0.02		W9	Internal conversion in $Pb^{212}-Bi^{212}-Tl^{208}$
83 Bi				0.40±0.02			(ThB−C−C″).

[a] See list at end of article.

degrees of forbiddenness, Brosi, Ketelle, Thomas, and Kerr concluded that the capture transition is forbidden, and used the fact in the further elucidation of their decay scheme.

V. SUMMARY OF DATA ON MEAN L-FLUORESCENCE YIELDS

The determination of mean L-fluorescence yields was discussed in reference 1, and a more recent summary has been given by Fink (F5). Since that time additional measurements have appeared from studies on radioactive Tb, Yb, Hf, Au, Hg, Tl, Pb, and Bi. Roos (R6) has informed us of the results of x-ray excitation experiments on Ta, Pt, Au, and Pb. Lazar (L15) has also made recent measurements of the ratio of the K_α and K_β x-ray intensities. These new results are summarized in Table V; and these values, as well as all other available nuclear data on ω_L, are shown in Fig. 5, in which the values obtained by Lay (L14) for x-ray excitation are shown for comparison. The break at $Z\approx 73$ is interpreted to mean that above this point Coster-Krönig transitions of the type $L_\text{I}-L_\text{III}M_\text{IV,V}$ contribute, thus shifting L_I vacancies to the L_III subshell for which the partial fluorescence yield is greater. These transitions are energetically forbidden for $Z \lesssim 73$, and other Coster-Krönig transitions which transfer vacancies between the L subshells occur only to a very small extent.[30]

As pointed out previously,[1] the mean L-fluorescence yield is an average of the fluorescence yields of the L subshells, weighted in a manner which is not at all well known, and weighted differently for different modes of excitation. Ross, Cochran, Hughes, and Feather[31] analyzed this problem in very great detail, and extracted the partial L-fluorescence yields for bismuth from experimental results on x-ray fluorescence excitation and on nuclear excitation by internal conversion of the 47-kev gamma ray of RaD(Pb^{210}). This analysis is summarized briefly by Wapstra, Nijgh, and Van Lieshout.[4] Unfortunately there is very little detailed data except in the region around $Z=82$, and we can only echo the call[31] for more precise and more extensive experimental measurements in this field.

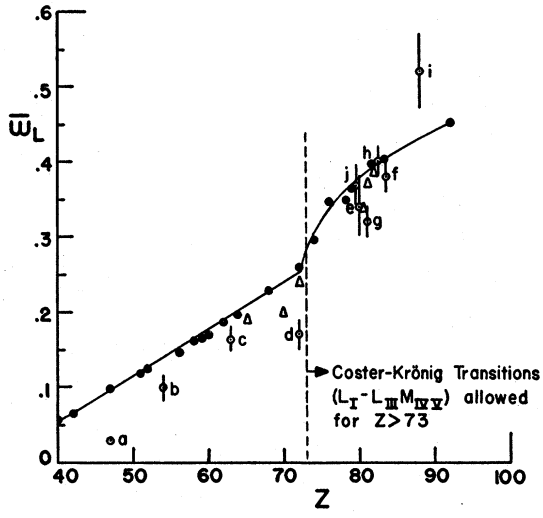

FIG. 5. Mean L-fluorescence yields *vs* atomic number. The solid points are the results of Lay (L14) from x-ray excitation. Open points are all derived from nuclear excitation and represent the following work (see list of references at end of article): (*a*) Ag^{109}, from *EC* in Cd^{109} (B3), (*b*) Xe^{131}, from *EC* in Cs^{131} (F3), (*c*) Eu^{153}, from decay of Gd^{153} (B13), (*d*) Hf^{179}, from *EC* in Ta^{179} (B15), (*e*) Hg^{204}, from *EC* in Tl^{204} (S10), (*f*) Bi^{210}, from decay of Pb^{210} (RaD) (F5), (*g*) Tl^{208}, from alpha decay of Bi^{212}(ThC) (W9) (see also B22), (*h*) Bi^{212}, from decay of Pb^{212}(ThB) (W9) (see also B22), (*i*) Ra^{226}, from alpha decay of Th^{230}(Io) (B23), (*j*) Hg^{199}, from decay of Au^{199} (H16). Open triangles are the data from (L15).

[30] E. H. S. Burhop, *The Auger Effect* (Cambridge University Press, Cambridge, England, 1954).

[31] Ross, Cochran, Hughes, and Feather, Proc. Phys. Soc. (London) **A68**, 612 (1955).

CODED REFERENCES FOR TABLES I–V AND FIG. 5

B3. Bertolini, Bisi, Lazzarini, and Zappa, Nuovo cimento **11**, 539 (1954).
B5. Bisi, Terrani, and Zappa, Nuovo cimento **1**, 651 (1955).
B13. Bisi, Germagnoli, and Zappa, Nuclear Phys. **1**, 593 (1956).
B15. Bisi, Zappa, and Zimmer, Nuovo cimento **4**, 307 (1956).
B17. Bisi, Germagnoli, and Zappa, Nuovo cimento **6**, 299 (1957).
B18. S. K. Bhattacherjee and S. Raman, Nuclear Phys. **1**, 486 (1956). There appears to be an arithmetic error in the calculation on pages 494–495. Recalculation gives $\epsilon=0.74 \pm 0.26$.
B22. J. Burde and S. G. Cohen, Phys. Rev. **104**, 1085 (1956).
B23. Booth, Madansky, and Rasetti, Phys. Rev. **102**, 800 (1956).
B24. Bhatki, Gupta, Jha, and Madan, Nuovo cimento **6**, 1461 (1954).
B25. Brosi, Ketelle, Thomas, and Kerr, Phys. Rev. **113**, 239 (1959).
B26. Bisi, Zappa, and Germagnoli, Nuovo cimento **4**, 764 (1956).
B27. Bisi, Germagnoli, and Zappa, Nuovo cimento **11**, 843 (1959).
C5. Cork, Nester, LeBlanc, and Brice, Phys. Rev. **92**, 119 (1953).
D6. R. W. P. Drever and A. Moljk, Phil. Mag. **2**, 427 (1957).
D7. Drever, Moljk, and Curran, Nuclear Instr. **1**, 41 (1957).
D8. DeBrunner, Heer, Kundig, Ruetschi, and Lindquist, Helv. Phys. Acta **29**, 235, 432, 463 (1956) [see p. 501].
D9. R. W. P. Drever (private communication 1959).
E2. Elwyn, Landon, Oleska, and Glasoe, Phys. Rev. **112**, 1200 (1958).
F3. R. W. Fink and B. L. Robinson, Phys. Rev. **98**, 1293 (1955).
F5. R. W. Fink, Phys. Rev. **106**, 266 (1957).
F6. B. M. Foreman, Jr., and G. T. Seaborg, J. Inorg. Nuclear Chem. **7**, 305 (1958).
G6. P. R. Gray, Phys. Rev. **101**, 1306 (1956).
G7. R. K. Gupta and S. Jha, Nuovo cimento **5**, 1524 (1957).
G8. Gindler, Huizenga, and Engelkemeir, Phys. Rev. **109**, 1263 (1958).
G9. R. K. Gupta, Proc. Phys. Soc. (London) **71**, 330 (1958).
G10. Gupta, Jha, Joshi, and Madan, Nuovo cimento **8**, 48 (1958).
G11. Grigor'ev, Kusnetzov, Shimanskaya, and Yutlandov, Izvest. Akad. Nauk SSSR, Ser. Fiz. **22**, 850 (1958); Chem. Abstracts **52**, 19559g (1958), Nuclear Sci. Abstr. **13**, 5032 (1959).
G12. R. K. Gupta and S. Jha, Nuovo cimento **4**, 88 (1956).
G13. C. F. Giese and J. L. Benson, Phys. Rev. **110**, 712 (1958).
H4. J. Heintze, Z. Naturforsch. **9a**, 469 (1954).
H5. J. R. Huizenga and C. M. Stevens, Phys. Rev. **96**, 548 (1954).
H8. R. W. Hoff, University of California Radiation Laboratory Rept. UCRL-2325 (1954) (unpublished).
H10. Hoff, Olsen, and Mann, Phys. Rev. **102**, 805 (1956).
H13. Hamers, Marseille, and DeBoer, Physica **23**, 1056 (1957).
H14. D. C. Hoffman and B. J. Dropesky, Phys. Rev. **109**, 1282 (1958).
H15. R. E. Holland and F. J. Lynch, Phys. Rev. **113**, 903 (1959).
H16. S. K. Haynes and W. T. Achor, J. phys. et radium **16**, 635 (1955).
J4. R. G. Jung and M. L. Pool, Bull. Am. Phys. Soc. **1**, 172, E11 (1956).
J5. Johns, Nablo, and King, Can. J. Phys. **35**, 1159 (1957).
J6. Johansson, Cauchois, and Siegbahn, Phys. Rev. **82**, 275 (1951).
K4. Ketelle, Thomas, and Brosi, Phys. Rev. **103**, 190 (1956).
K8. S. Katcoff, Phys. Rev. **111**, 575 (1958).
K9. Koertz, Macklin, Farrelly, van Lieshout, and Wu, Phys. Rev. **98**, 1230 (1955).
K10. R. W. Kiser and W. H. Johnston, J. Am. Chem. Soc. **81**, 1810 (1959).
K11. B. H. Ketelle and A. R. Brosi, Phys. Rev. **116**, 98 (1959).
L11. M. Langevin and P. Radvanyi, Compt. rend. **241**, 33 (1955).
L12. M. Langevin, J. phys. et radium **16**, 516 (1955); Ann. phys. **10**, 584 (1955).
L14. H. Lay, Z. Physik. **91**, 533 (1934).
L15. N. H. Lazar and W. S. Lyon, Bull. Am. Phys. Soc. **3**, 29, K10 (1958) and (private communication, February 28, 1958).
M4. E. der Mateosian and A. Smith, Phys. Rev. **88**, 1186 (1952).
M5. E. der Mateosian, Phys. Rev. **92**, 938 (1953).
M12. A. Moussa and A. Juillard, Compt. rend. **243**, 1515 (1956).
M13. Magnusson, Friedman, Engelkemeir, Fields, and Wagner, Phys. Rev. **102**, 1097 (1957).
M15. N. Marty and M. Vergnes, Compt. rend. **242**, 1438 (1956).
M16. C. W. McCutchen, Nuclear Phys. **5**, 187 (1958).
N1. R. A. Naumann, Bull. Am. Phys. Soc. **1**, 42, K9 (1956).
O2. Olsen, Mann, and Lindner, Phys. Rev. **106**, 985 (1957); Bull. Am. Phys. Soc. **1**, 41, K2 (1956).
R6. C. E. Roos (private communication 1959).
S9. J. Scobie, Nuclear Phys. **3**, 465 (1957).
S10. H. Schmied and R. W. Fink, Phys. Rev. **107**, 1062 (1957).
S12. J. Scobie and E. Gabathuler, Proc. Phys. Soc. (London) **72**, 437 (1958).
S13. Scobie, Moler, and Fink, Phys. Rev. (submitted for publication).
S14. Strominger, Hollander, and Seaborg, Revs. Modern Phys. **30**, 585 (1958).
T3. W. Turchinetz and W. R. Pringle, Phys. Rev. **103**, 1000 (1956).
W4. A. H. Wapstra and W. Van der Eijk, Nuclear Phys. **4**, 325 (1957).
W5. Wing, Stevens, and Huizenga, Phys. Rev. **111**, 590 (1958).
W6. J. Welker and M. L. Perlman, Phys. Rev. **100**, 74 (1955).
W7. Way, King, McGinnis, and van Lieshout, *Nuclear Level Schemes*, U. S. Atomic Energy Commission Rept. TID 5300 (U. S. Government Printing Office, Washington 25, D.C., 1955).
W8. C. L. McGinnis, Editor, *Nuclear Data Sheets* (National Academy of Sciences, National Research Council, Washington D. C., 1958).
W9. H. Winkenbach, Z. Physik **152**, 387 (1958).